



Effect of Electromagnetic Bandgap Structures on Performance of Planar Textile Antenna

Wasi U.R. Khan¹, Sadiq Ullah^{1*}, Syed M. Umar¹, Shahid Bashir², and Farhan Ahmad¹

¹Department of Telecommunication Engineering, University of Engineering and Technology, Peshawar, Pakistan

²Department of Electrical Engineering, University of Engineering and Technology, Peshawar, Pakistan

Abstract: The paper introduces a comparative analysis of a wearable, metamaterial based 2.4 GHz microstrip patch antenna using three variants of Electromagnetic Bandgap (EBG) ground planes. A 1.8 mm thick wearable fabric (Velcro) having relative permittivity of 1.34 and tangent loss of 0.006 is used as a substrate material in the design of the conventional antenna and EBG ground planes. Three types of unit cells, namely, mushroom, slotted cross and slotted I are proposed to design the EBG ground planes. The antenna using slotted cross shape EBG as a ground plane is more compact (having 16 % reduced size) as compared to the rest of the three. The conventional antenna without EBG ground plane is relatively least efficient (77.53 %) with a gain of 8.14 dB. The same antenna if backed by a mushroom type EBG, radiate efficiently (80.92 %) with a gain of 9.63 dB in the boresight direction. The wearable antenna and EBG ground planes are designed, characterized and numerically analyzed using the Finite Integration Technique (FIT). These antennas can be used in sports, military, medical, security and rescue applications.

Keywords: Wearable, Metamaterial, Patch antenna, EBG

1. INTRODUCTION

Antenna is a vital component of any wireless communication system which converts the electric signal into electromagnetic wave; therefore, it must meet the criteria of being optimally efficient, compact and broadband. Microstrip patch antennas because of their easy fabrication, low cost, conformability, light weight and low profile planar configuration are suitable candidates. However, patch antennas have the limitations of low gain, low efficiency and narrow bandwidth [1-4], if not properly designed. Several techniques have been proposed in the past for enhancing the bandwidth of patch antennas, including use of a thick substrate material [5]. However, thick substrate results in excitation of surface waves within it. These waves propagate within the substrate, get scattered at the edges and degrade the radiation pattern. This phenomenon

also reduces the efficiency and gain of the patch antenna along the boresight direction. In order to resolve the limitations of thick substrate antennas researchers have proposed different techniques. One of the technique is the metamaterial based Electromagnetic Bandgap (EBG) structures [6-7]. Surface wave suppression and in-phase reflection are the characteristic electromagnetic properties of Electromagnetic Band (EBGs) structures as compared to traditional substrates and metallic ground planes [8].

In case of normal incident plane wave, Perfect electric conductor (PEC) has a reflection phase of 180° and Perfect magnetic conductor (PMC) which does not exist in nature has 0° reflection phase. Much endeavors have been devoted to design PMC-like surfaces, and it has been found that EBG structures can satisfy the PMC-like condition in

a particular frequency band. The reflection phase of an EBG surface is not fixed like PEC or PMC surface but it shifts continually from -180° to 180° versus frequency. This reflection phase behavior makes EBG surfaces one of a kind [9].

Electromagnetic bandgap ground structure acts like 2D parallel LC-resonating circuit. The resonant frequency of the EBG surface is thus controlled by inductance and capacitance which is dependent on the geometry of EBG unit cell [10]. At the resonating frequency the impedance of the EBG surface is very high and the propagation of surface waves is prohibited in all direction. This phenomenon is known as surface wave suppression which makes an antenna efficient. EBG structures have been used as an antenna ground plane in a variety of wireless applications including fixed, land mobile, satellite, cellular and wearable electronics [11-14].

As EBG based antenna is large in size compared to patch antenna without EBG ground plane so it has been a limitation of EBG structures to incorporate them with wearable antennas. Miniaturized EBG structures have been proposed by many researchers for portable wireless applications [15-20].

Miniaturization of EBG based patch antenna can be accomplished by using various size reduction techniques. The technique that is used here is by inserting slots which shifts down the frequency of the EBG unit cell which in turn reduces the size of EBG based patch antenna.

This paper compares the performance of a conventional 2.4 GHz microstrip wearable patch antenna with three different EBG based wearable patch antennas using Velcro as a substrate material. The paper presents two modified and miniaturized forms of mushroom type EBG structures i.e. Slotted-I and slotted-cross, both are used as a ground plane for the proposed wearable patch antenna. This paper is organized as follows. Section 2 describes the design procedure of antenna. Section 3 explains design methodology of EBG structures. Section 4 explains the salient results and related discussion. Finally, section 5 gives the conclusion of this research paper.

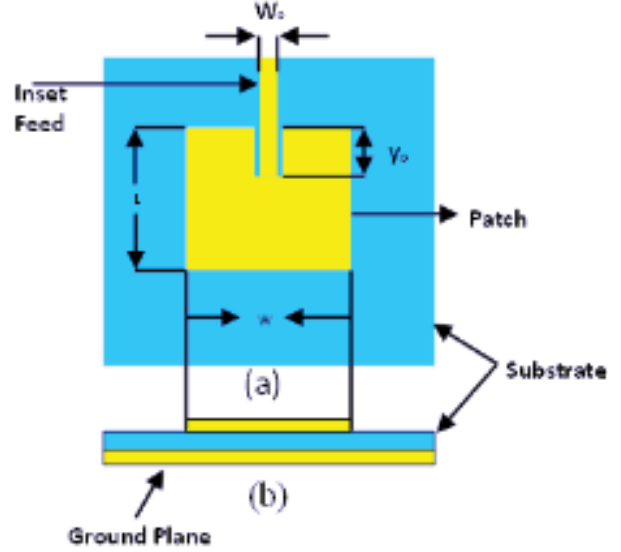


Fig. 1. Geometry of a conventional wearable patch antenna: (a) Front view; (b) Side view.

2. DESIGN METHODOLOGY OF CONVENTIONAL WEARABLE PATCH ANTENNA

The structure of proposed patch antenna is depicted in Fig. 1. Wearable material Velcro having a permittivity of 1.34 and tangent loss of 0.006 respectively, is used as a substrate. The dimensions of the patch {length (L), width (W)}, and inset feed {position (y_0), width (w_0)} for the resonant frequency (f_r) are calculated using the following fundamental equations [4]:

$$W = \frac{c}{2 f_r} \sqrt{\frac{2}{\epsilon_r + 1}} \quad (1)$$

$$L = \frac{c}{2 f_r \sqrt{\epsilon_{reff}}} - 2\Delta L \quad (2)$$

Where, c is the speed of light in vacuum, ϵ_{reff} is the effective relative permittivity of the substrate of thickness (h) and ΔL the differential increase in resonant length due to fringing.

$$\epsilon_{reff} = \frac{\epsilon_r + 1}{2} + \frac{\epsilon_r - 1}{2} \left[1 + 12 \frac{h}{W_p} \right]^{-1/2} \quad (3)$$

$$\frac{\Delta L}{h} = 0.412 \frac{(\epsilon_r + 0.3) \left(\frac{W}{h} + 0.264 \right)}{(\epsilon_r - 0.258) \left(\frac{W}{h} + 0.8 \right)} \quad (4)$$

The position of the feed (y_0) is found using the relationship between the input resistances at 50 Ω feed point ($R_{in}(y=y_0)$) and edge of the patch ($R_{in}(y=0)$). The later varies in the range of 200-300 Ω and depends on the conductance (G_p) of the patch.

Table 1. Summary dimensions of wearable patch antenna (Fig. 1)

| Parameter | Calculated (mm) | Optimized (mm) |
|--------------------------|-----------------|----------------|
| Length (L) | 52.27 | 52.27 |
| Width of patches (W) | 57.75 | 57.78 |
| Inset feed position (yo) | 17.67 | 17.67 |
| Feed width (wo) | 8.12 10 | |

Table 2. Summary of the three EBG unit cells.

| Type | Width (W) (mm) | Gap (g) (mm) | Via (mm) | Periodicity, a (mm) | Reduction |
|---------------|-------------------|-----------------|-------------|------------------------|----------------|
| Mushroom | 44 | 0.8 | 1 | 44.8 | 0% (Reference) |
| Slotted I | 37.7 | 0.8 | 1 | 38.5 | 14.31% |
| Slotted cross | 37 | 0.8 | 1 | 37.8 | 15.9% |

It can be found using the transmission line model of patch antennas, i.e.

$$R_{in}(y = yo) = R_{in}(y = 0) \cos^2\left(\frac{\pi}{L} yo\right) \quad (5)$$

$$R_{in}(y = 0) \approx \frac{1}{2G_1} \quad (6)$$

$$G_1 = \frac{1}{90} \left(\frac{W}{\lambda_0}\right)^2 \quad (7)$$

The width of the feed line (W_0) is found using [4]

$$W_0 = \left(\frac{377}{Z_c \sqrt{\epsilon_r}} - 2\right) h \quad (8)$$

Where, Z_c is the characteristic impedance of the feed line. The calculated dimensions were optimized for the desired radiation characteristics at 2.4 GHz and are given in Table 1.

3. DESIGN METHODOLOGY OF WEARABLE EBG STRUCTURES

Electromagnetic bandgap ground structures are widely used as ground plane in antenna design for improving its radiation characteristics (gain, directivity, efficiency). In this section three variants of EBG structures (slotted-cross, slotted-I, and mushroom), each employing Velcro as a substrate material, are designed. These structures are characterized in terms of their surface wave and in-phase reflection bandgap capabilities. The overall performance of proposed patch antenna with the conventional ground plane replaced by these EBG

surfaces is also compared.

Geometry of Electromagnetic Bandgap Ground Structure

The basic theory of periodic EBG [7] is used to design the proposed EBG ground planes. The resonant frequency (f_r) and bandwidth (BW) of the unit cells of the EBG structures is evaluated in terms of electrical parameters i.e. capacitance (C) and inductance (L) as follows:

$$f = \frac{1}{2\pi\sqrt{LC}} \quad (9)$$

$$BW = \frac{1}{\eta_0} \sqrt{\frac{L}{C}} \quad (10)$$

Where, η_0 is the intrinsic impedance of free space (377Ω). The electrical parameters (L , C) are dependent on the unit cells geometry as well as the substrate material being used.

$$L = \mu_o \mu_r h \quad (11)$$

$$C = 2w \epsilon_o \frac{(1+\epsilon_r)}{\pi} \cosh^{-1} \frac{(w+g)}{g} \quad (12)$$

Where, w and g are the width of the EBG unit cell's patch and gap between the neighboring cells respectively. The geometry of the unit cells of mushroom, slotted-I and slotted-cross EBG structures is depicted in Fig. 2(a), 2(b) and 2(c), respectively.

The resonant frequency and the transmission

characteristics of these structures depend on the overall geometry of the unit cell and the substrate material being used. In other words, the resonant frequency, surface wave bandgap and in-phase reflection of these structures takes into account type of the substrate material, the thickness and width (w) of the metal patch, diameter of via and the gap (g) between the neighboring patches [9]. Alternatively, the electromagnetic behavior of the EBG structures depend on the periodicity ($a=w+g$) of the structure and substrate material. In this paper 1.8 mm thicker Velcro is used as a substrate material for the three surfaces. The optimized dimensions of the three unit cells (Fig. 2) are summarized in Table 2.

4. RESULTS

4.1 In-phase reflection

In-phase reflection is one of the unique feature of EBG structures, which decides if the structure is working as a Perfect Magnetic Conductor (PEC) at the design frequency or as an (AMC) Artificial Magnetic Conductor within a certain frequency band (known as in-phase reflection bandwidth, BW_{ipr}). The reflection phase of the EBG surface within this bandwidth shifts from $+90^\circ$ to -90° crossing through 0° at the center frequency (f_r). The following equation is used to evaluate the bandwidth:

$$BW_{ipr} = \frac{f_{-90} - f_{90}}{f_r} \times 100 \quad (13)$$

Where f_{-90} and f_{90} are the higher and lower frequencies belonging to -90° and 90° reflection phases respectively. The reflection phase of the EBG unit cells is simulated by illuminating it with plane wave being incident from $+Z$ direction and using the periodic boundary conditions as illustrated in Fig. 3.

The reflection phase response of three different EBGs structures is depicted in Fig. 4. As can be seen the reflection phase bandwidth of the mushroom, slotted-I and slotted-cross type EBG structures is 8.9%, 7.2% and 6 %, respectively.

4.2 Surface Wave Bandgap

The frequency range within which the EBG

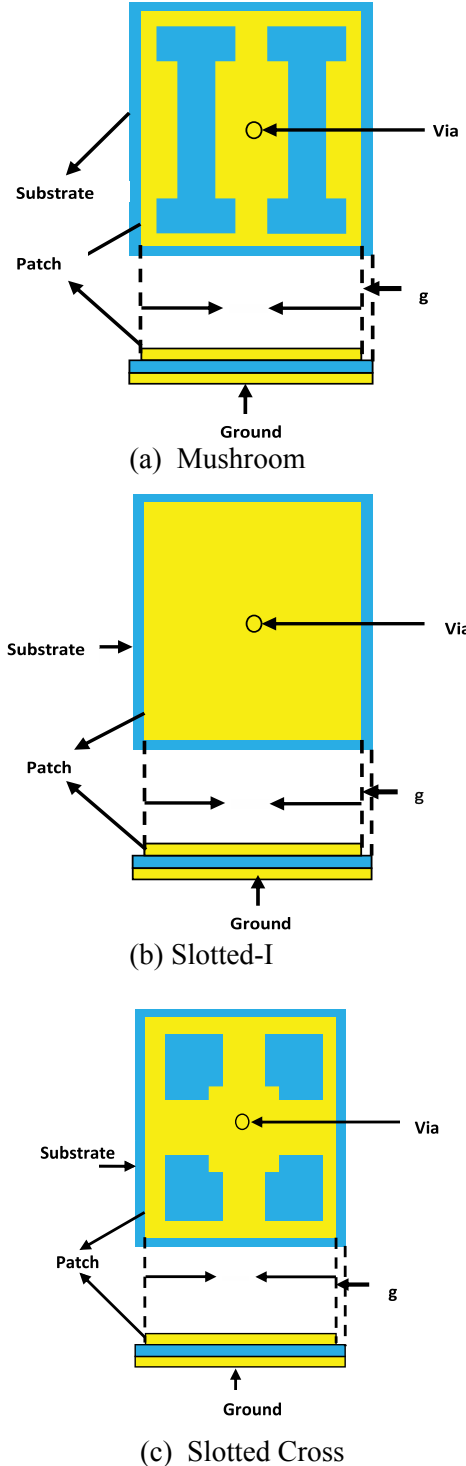


Fig. 2. Unit cells of EBG surfaces.

suppresses the propagation (or transmission) of surface waves within the substrate is known as the surface wave bandgap. The setup in Fig. 5 is used to investigate the transmission characteristics of the three EBG surfaces, each 3 x 3 unit cells in size.

A 50 ohm microstrip line of width (4 mm) is

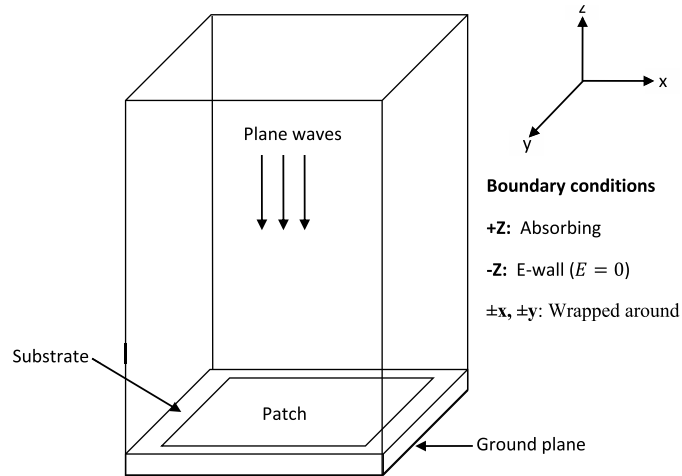


Fig. 3. Setup for in-phase reflection of EBG surface.

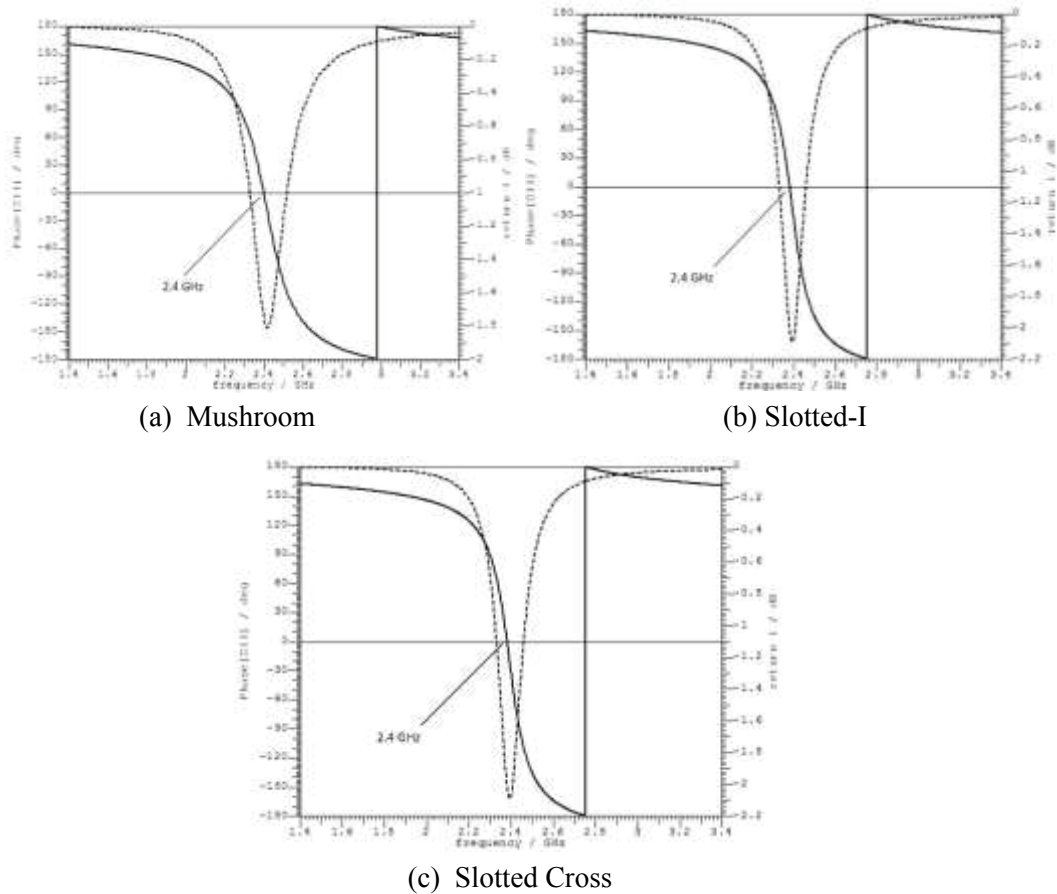


Fig. 4. Reflection phase of Velcro-based EBG surfaces.

fixed at a height of 0.035 mm above each surface and it was excited at both ends using waveguide ports. The width of the line is evaluated using the standard transmission line theory.

The transmission coefficients ($S_{21} = S_{12}$) of the three surfaces are analyzed and compared in Fig. 6. It is evident that in the 2.4 GHz bandwidth none of the three surfaces give surface wave suppression. It

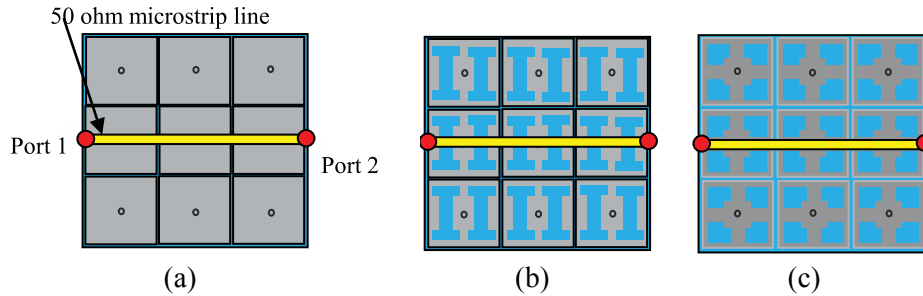


Fig. 5. Setup for Bandgap characterization of EBG surfaces (each 3 x 3 unit cells in size): (a) Mushroom; (b) Slotted 1 (C) Slotted cross.

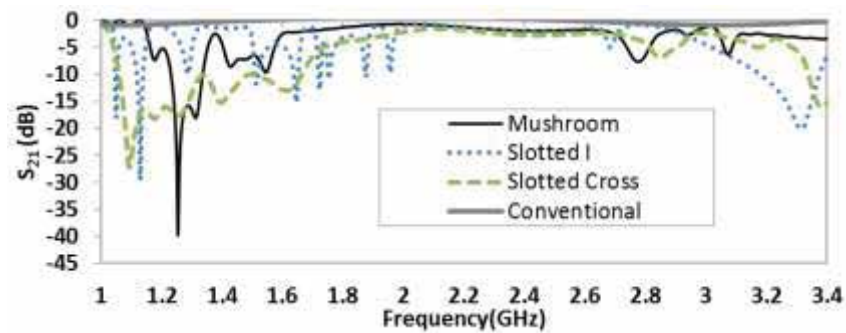


Fig. 6. Transmission parameter of the proposed EBG surfaces.

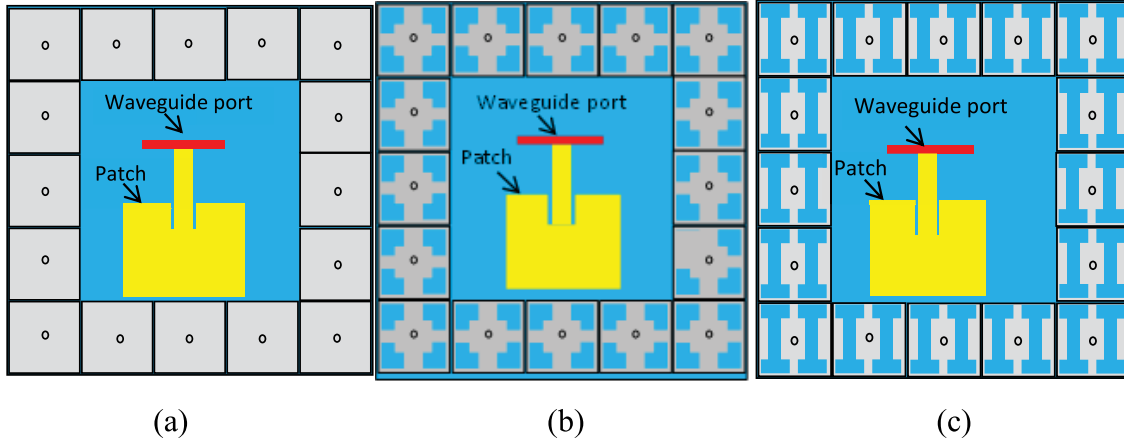


Fig. 7. Design of 2.4 GHz wearable patch antenna using EBG ground plane: (a) Mushroom; (b) Slotted Cross; (c) Slotted I.

is worth noticing that these surfaces show surface wave bandgap in lower frequency bands 1.1-1.4 GHz which can be utilized in the design of efficient antennas in these bands.

4.3 Characterization and Analysis of Wearable Antenna

In this section, the radiation characteristics of the

2.4 GHz wearable patch antenna is analyzed using conventional conductor ground plane and three EBG ground planes. The proposed patch antenna is mounted on an appropriate position within the available space by removing the top layer of the nine unit cells from the center of the Electromagnetic Band Gap plane (Fig. 7). The proposed antenna is excited through a waveguide port and analyzed in the 1.4-3.4 GHz frequency range.

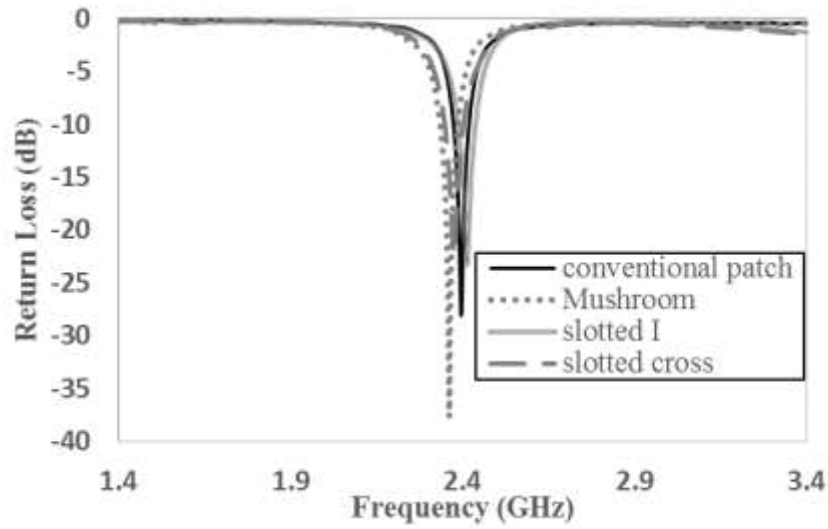


Fig. 8. Return loss comparison of the proposed antenna on different ground planes.

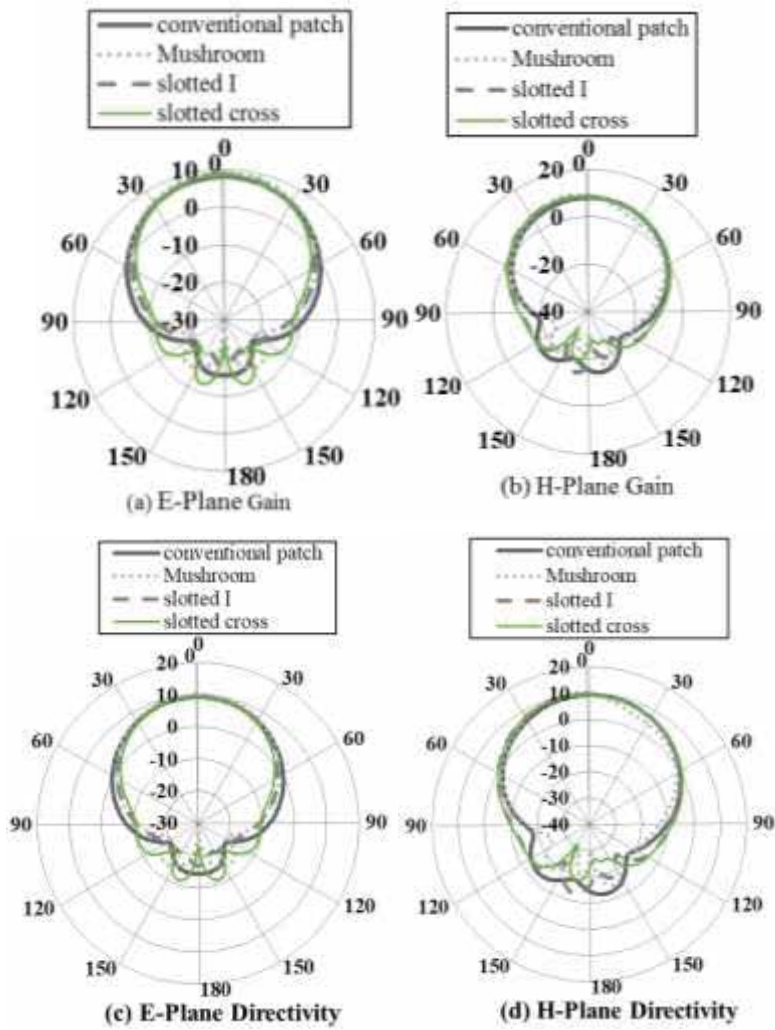


Fig. 9. Gain and directivity of 2.4 GHz wearable antenna on various ground planes.

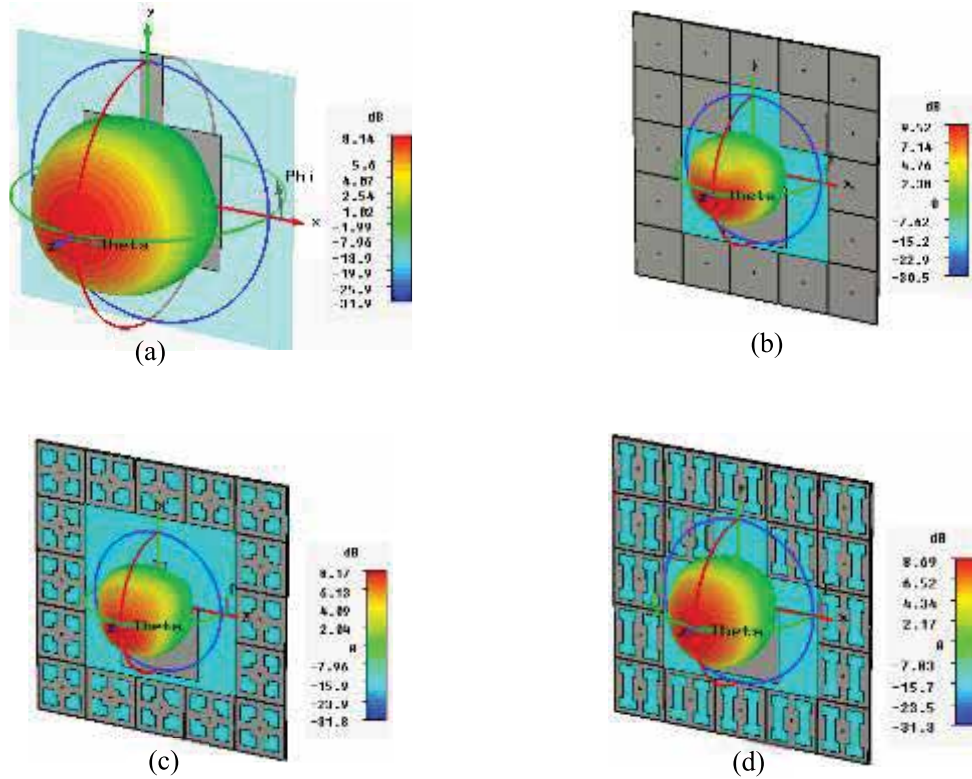


Fig. 10. Perspective view of three-Dimensional gain plots of the patch antenna on different ground planes: (a) Conventional; (b) Mushroom; (c) Slotted-cross; (d) Slotted-I.

Table 3. Summary of results of proposed wearable patch antenna on various ground planes.

| Parameter/Ground Plane | Conventional | Mushroom | Slotted I | Slotted cross | |
|------------------------|--------------|----------|-----------|---------------|-------|
| Frequency (GHz) | 2.394 | 2.36 | 2.41 | 2.376 | |
| Return loss (dB) | -28.04 | -37.682 | -23.32 | -22.35 | |
| Bandwidth(MHz) | 45.5 | 50.8 | 52.4 | 59.5 | |
| Beamwidth (Degrees) | $\phi=00$ | 67.5 | 65.3 | 59.7 | 61 |
| | $\phi=900$ | 68.1 o | 39.3 | 63.2 | 59.2 |
| Side Lobe Level (dB) | $\phi=00$ | -23.5 | -24.1 | -26.3 | -20.2 |
| | $\phi=900$ | -22 | -25.5 | -23.3 | -22.6 |
| Gain (dBi) | 8.143 | 9.630 | 8.683 | 8.713 | |
| Directivity(dB) | 9.24 | 10.55 | 9.632 | 9.592 | |
| Efficiency (%) | 77.53 | 80.92 | 80.40 | 81.66 | |

The return loss of the proposed antenna on the conventional ground plane and EBG ground planes(mushroom, slotted-I and slotted-cross) is compared in Fig. 8 .It shows that the proposed antenna gives prominent resonance near the design frequency (2.4 GHz) independent of the sort of the ground plane being utilized. The slight shift in the

resonant frequency is because of the minor change in the effective electrical properties (capacitance and inductance) of the patch antenna due to the EBG ground plane.

The E-plane ($\phi=0^\circ$) radiation pattern of the proposed antenna on these different ground planes

is compared in Fig. 9(a). The proposed patch antenna with slotted cross EBG ground plane shows higher (-20.2 dB) side lobe radiations whereas the slotted-I EBG antenna shows lowest side lobe radiations (-26.3 dB) in this plane. The gain of the antenna is 8.143dB, 9.63dB, 8.68dB and 8.71dB dB with conventional ground, EBG (i.e. mushroom, slotted-I and slotted-cross) ground planes respectively. The conventional antenna possesses the highest 3 dB beamwidth (67.5°) whereas the mushroom EBG antenna has the lowest beamwidth (39.3°) in this plane.

The H-plane ($\phi=90^\circ$) gain of the proposed antenna is compared on these ground planes in Fig. 9(b). The proposed antenna without EBG ground plane shows relatively higher back lobe levels and side lobes. The 3 dB beamwidth of the conventional antenna is relatively broader (68.1°) while that of mushroom based antenna is narrower (39.3°) in the H-plane. The directivity of the proposed antenna on various ground planes has been evaluated in both the principal planes (E and H) as shown in Fig. 9(c) and Fig. 9(d). It is evident that the shape of the directivity pattern is identical to the respective gain pattern except the values are slightly higher due to the fact that directivity does not take into account the losses within the structure of the antenna and is purely dependent on the far-field radiation pattern.

Comparatively, the conventional antenna has the lowest gain (8.143 dBi) and efficiency (77.53 %). The gain of the EBG based antennas is relatively enhanced due to the AMC behavior of the EBG ground planes in the desired 2.4 GHz band. The mushroom type EBG based antenna has relatively higher gain (9.63 dBi) and efficiency (80.92 %). For further clarification of the boresight gain, side and back lobe radiation, the three-dimensional gain patterns of the proposed 2.4 GHz patch antenna on various ground planes are illustrated in Fig. 10.

The performance parameters of the proposed antenna backed by these ground planes are summarized in Table 3.

5. CONCLUSIONS

In this study microstrip patch antenna on conventional ground plane and three different

EBG ground planes were simulated, analyzed and compared with respect to gain, directivity, efficiency, beamwidth and return loss. The performance of antenna improves due to PMC like behavior of EBG structures. The gain was increased to 9.6dBi as compared to 8.1dBi for conventional ground plane. In order to decrease the size three different EBG structures were studied and it was found that slotted cross EBG results into 16% reduction in size as compared to mushroom type EBG. These EBG based antennas can be used in portable wireless communication systems.

6. REFERENCES

1. Ali, U., S. Ullah, S. Khan, J.A. Flint. Comparative study of rectangular microstrip patch antenna on various types of metamaterial surfaces. In: *Proceedings of International Conference on Open Source Systems and Technologies (ICOSST)*, p. 186-191 (2014).
2. Savita, M.S., R.M. Vani, R.T. Prashant, & P.V. Hunagund. Design of rectangular microstrip antenna with EBG for multiband operations. *International Journal of Application or Innovation in Engineering & Management* 3: 127-132 (2014).
3. Helena, D., M.R. Margaret, S. Subasree, S. Susithra, Keerthika, & B. Manimegalai. Comparison of compact EBG structures on the mutual coupling reduction of antenna arrays. *International Journal of Future Computer and Communication* 2: 76-79 (2014).
4. Balanis, C.A. *Antenna Theory: Analysis and Design*, 2nd ed. John Wiley & Sons, Singapore (1997).
5. Kovitz, J.M., & Y. Rahmat-Samii. Using thick substrates and capacitive probe compensation to enhance the bandwidth of traditional CP patch antennas. *IEEE Transactions on Antennas and Propagation* 62(10): 4970-4979 (2014).
6. Han, Z.J., W. Song, W.J. Li, & X.Q. Sheng. High-gain and low-profile EBG patch antenna design. In: *Proceedings 37th Progress in Electromagnetic Research Symposium*, 8-11 August, 2016, Shanghai, China, p. 1676-1679 (2016).
7. Han, Z.J., W. Song, & X.Q. Sheng. Gain enhancement and RCS reduction for patch antenna by using polarization-dependent EBG surface. *IEEE Antennas and Wireless Propagation Letters* 99: 1-1 (2017).
8. Wu, J., S. Yang, Y. Chen, S. Qu, & Z. Nie. A Low Profile dual-polarized wideband omnidirectional antenna based on AMC reflector. *IEEE Transactions on Antennas and Propagation* 65(1): 368-374 (2017).

9. Yang, F., & Y. Rahmat-Samii. Reflection phase characterizations of the EBG ground plane for low profile wire antenna applications. *IEEE Transaction on Antennas and Propagation* 51(10): 2691-2703 (2003).
10. Afridi A, S. Ullah, S. Khan, A. Ahmed, A.H. Khalil, M.A.Tarar. Design of dual band wearable antenna using metamaterials. *Journal of Microwave Power and Electromagnetic Energy* 47(2):126-37 (2013).
11. Kushwaha, N., & R. Kumar. Study of different shape electromagnetic band gap (EBG) structures for single and dual band applications. *Journal of Microwaves, Optoelectronics and Electromagnetic Applications* 1: 111-122 (2014).
12. Rezaei M.R., & P. Rezaei. Design of a novel EBG structure and its application for improving performance of a low profile antenna. In: *Proceedings Iranian Conference on Electrical Engineering (ICEE)*, 17-19 May 2011, Tehran, Iran, p. 1-5 (2011).
13. Yang, F., & Y. Rahmat-Samii. *Electromagnetic Band Gape Structures in Antennas*, 1st ed. Cambridge University Press (2008).
14. Rahmat-Samii, Y., & H. Mosallaei. Electromagnetic band-gap structures: Classification, characterization and applications. *11th International Conference on Antennas and Propagation (ICAP 2001)*, 17-20 April 200, Manchester, UK, p. 560-564 (2001).
15. Yang, L., M. Fan, F. Chen, J. She, & Z. Feng. A novel compact electromagnetic-bandgap (EBG) structure and its applications for microwave circuits. *Microwave Theory and Techniques, IEEE Transactions* 53: 183-190 (2005).
16. Md. Shahid ul-Alam, M., & M. Tariq ul Islam. Development of electromagnetic bandgap structures in the perspective of microstrip antenna design. *International Journal of Antennas and Propagation* 1: 1-22 (2013).
17. Yan, Z., & Y. Wang. A novel miniaturized electromagnetic bandgap structure and its effects on signal integrity and electromagnetic emission. *International Journal of Antennas and Propagation* 1: 1-7 (2013).
18. Shaka, S.M., R.T. Prashant, R.M. Vani, & P.V. Hunagund. Study of microstrip antenna using various types of EBG cells. *International Journal of Advanced Research in Electrical, Electronics and Instrumentation Engineering* 3: 9680-9685 (2014).
19. Khadim Ullah Jan, Shahid Bashir. Compact size EBG with wider band gap and scalable features for printed antenna and arrays. *IEEE 9th International Conference on Emerging Technologies (ICET)*: 1-5 (2013).
20. Xie, H.-H, Y. Jiao, K. Song, & B. Yang. Miniature electromagnetic band gap structure using spiral ground plane. *Progress in Electromagnetics Research Letters* 17: 163-170 (2010).